

# Adaptive Two-Time-Scale Tracking Filter for Target Acceleration Estimation

Stephan A. R. Hepner and Hans P. Geering  
*Swiss Federal Institute of Technology, Zürich, Switzerland*

A critical phase during air-to-air interception is the homing phase. It is characterized by a short time to go and low bearing rates on the homing path. The phase is critical because any misconception with respect to the target maneuver may result in a substantial miss distance. This is essentially due to the lack of time to perform path corrections when the target produces a collision course error by an evasive maneuver. The estimation of the target acceleration is therefore crucial to the design of guidance laws that allow a fast response to target maneuvers. There are, however, severe problems associated with the synthesis of target trackers for air-to-air missiles. These problems include the lack of observability, modeling errors, and the restriction of the computation time due to high sampling rates. In this paper, a new tracking filter is presented that copes with the problems just mentioned. It is based on the time scale separation inherent in the tracking dynamics. In conjunction with a simple adaption scheme, this filter is able to track a large class of target maneuvers in a computationally efficient manner.

## I. Introduction

ESTIMATES of the current target acceleration are among the most important quantities that are required for the implementation of modern guidance laws for air-to-air missiles. These estimates are used either for the compensation of the target acceleration in simple extensions of proportional navigation<sup>17</sup> or for the prediction of the target maneuver, which is typically carried out in guidance algorithms based on optimal control theory. (For a survey, see Ref. 15.) The basic approach to the design of target acceleration estimators is the extended Kalman filter.<sup>3</sup> Essentially, there are three problems associated with target acceleration estimation in intercept applications.

1) The filter may diverge due to the lack of complete observability. It is well known that low observability always occurs when bearing angles or bearing rates are the only measurements available about the missile-target relative mo-

tion.<sup>1,10-12,15</sup> These measurements are common in short range missiles.

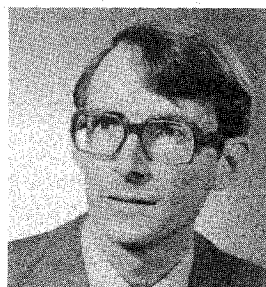
2) Since the exact dynamics of the target acceleration are unknown, assumptions must be made about the target behavior. The resulting modeling errors may cause the filter to diverge if no precautions are taken.

3) Since the changes of the target maneuver may be very fast, high sampling rates are required. Hence, the time to carry out the filtering computations is restricted to very short sampling intervals.

In this paper, a combination of tracking filter and guidance law is proposed that is able to cope with the problems just mentioned. It is robust with respect to estimation errors that result from low observability. It incorporates an adaption scheme that accounts for modeling errors in the target acceleration dynamics. It is computationally efficient because the estimation of the target acceleration is decoupled from the



Stephan A. R. Hepner received his M.S.M.E. and his Ph.D. degrees from the Swiss Federal Institute of Technology (ETH), Zürich, Switzerland, in 1982 and 1986, respectively. Presently, he is a Research Associate at the Measurement and Control Laboratory of ETH. His research interests are in nonlinear filtering theory, singular perturbation theory, optimal control, and adaptive control. He is a member of AIAA.



Hans P. Geering received his M.S.E.E. degree from the Swiss Federal Institute of Technology (ETH), Zürich, Switzerland, in 1966 and his Ph.D. degree from the Massachusetts Institute of Technology, Cambridge, MA, in 1971. He worked in the Military Division of Oerlikon-Buehrle Ltd. until he joined the faculty of the Department of Mechanical Engineering of ETH in 1979. Presently, he is a Professor of Automatic Control and Mechatronics. His research interests are in the areas of robust control and estimation with applications to automotive engine control and to navigation. He is a member of AIAA.

estimation of the missile-target relative motion (range and bearing angle dynamics). The approach is based on a time scale separation of the tracking dynamics. Although the concept of time scale separation has been applied extensively to the derivation of missile guidance laws, it has never been used to analyze the tracking problem. The separation of time scales is motivated by the observation that the missile and target heading dynamics are much faster than the dynamics of the bearing angle and the range. This allows for the construction of a low order, fast target acceleration estimator.

The remainder of this paper is divided into six sections. Section II contains the problem statement, the basic tracking algorithm, a summary of the main results on observability derived in Refs. 1 and 15, and the guidance law used in the simulations. An adaption algorithm that stabilizes the filter in the presence of certain modeling errors is presented in Sec. III. In Sec. IV, a scaled version of the tracking equations is suggested. An adaptive two-time-scale tracking filter based on the scaled tracking equations of Sec. IV is designed in Sec. V. Simulation results are presented in Sec. VI. A summary and conclusions are given in the last section.

## II. Problem Statement and Basic Tracking Algorithm

Consider the planar intercept problem depicted in Fig. 1. The scenario involves a short range air-to-air missile  $M$  and a highly maneuvering target  $T$ . Commonly  $M$  is equipped with a passive seeker providing bearing angle or bearing rate measurements. In the sequel, it will be assumed that bearing rate measurements are available. These measurements are the only information provided about the missile-target relative motion. The main goal is the synthesis of a tracking filter that supplies estimates of the target acceleration components to the guidance law of the missile. The basic approach is the extended Kalman filter (EKF).<sup>3</sup>

### Equations of the Tracking Problem

The design of an EKF requires models of the system dynamics, the measurement, and the noise statistics. Using the polar coordinates defined in Fig. 1, the following equations of relative motion of missile and target are obtained:

$$\ddot{\varphi} = (a_{T\varphi} - a_{M\varphi})/R - 2\dot{R}\dot{\varphi}/R \quad (1)$$

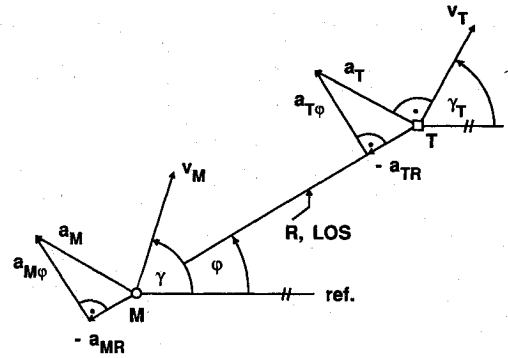
$$\ddot{R} = a_{TR} - a_{MR} + R\dot{\varphi}^2 \quad (2)$$

where the dotted quantities represent total derivatives with respect to time  $t$ . For the design of the tracking filter, it will be assumed that the missile accelerations  $a_{M\varphi}$  and  $a_{MR}$  can be measured precisely. In practice, a prefilter may be necessary to account for accelerometer noise. To complete the model [Eqs. (1) and (2)], the dynamics of the target accelerations  $a_{T\varphi}$  and  $a_{TR}$  must be formulated. In view of the restricted observability associated with bearing rate-only measurements, it is crucial to use all available knowledge about the target behavior when constructing a target model. The purpose is to exclude unrealistic target motion estimates a priori by appropriate assumptions. In short range scenarios involving aerodynamically controlled target aircraft, it is usually admissible to assume a constant target speed. Hence, the target acceleration is always directed normal to the target velocity (see Fig. 1). This results in the following target heading dynamics:

$$\dot{\gamma}_T = a_T/v_T \quad (3)$$

$$\ddot{\gamma}_T = \dot{a}_T/v_T \quad (4)$$

For a more detailed justification of this assumption, see Ref. 1. Notice that  $v_T$  is not a state of the target model, but a constant parameter. In the sequel, it will be assumed that this parameter is known (for example, from processing bearing and range data by the launching aircraft prior to firing the



M	: missile	T	: target
v	: velocity	a	: acceleration
LOS	: line of sight	R	: range
$\phi$	: bearing angle	$\gamma$	: heading angle

Fig. 1 Geometry of the planar tracking problem.

missile). Since the rate of change  $\dot{a}_T$  of the target acceleration is unknown,

$$\ddot{\gamma}_T = 0 \quad (5)$$

will be assumed for the design of the basic tracking algorithm. Notice that Eq. (5) is exact for constant-acceleration maneuvers, but modeling errors will occur when the target acceleration varies with time. In the latter case, an adaption scheme is required to stabilize the filter (see Sec. III). Defining the state vector

$$y^T = (\dot{\varphi}, \dot{R}, \varphi, R, \gamma_T, \dot{\gamma}_T) \quad (6)$$

where  $()^T$  denotes the transposed, the following state-space representation of the equations of motion is obtained from Eqs. (1-6):

$$\dot{y}_1 = \frac{v_T y_6 \cos(y_5 - y_3) - a_{M\varphi}}{y_4} - 2 \frac{y_1 y_2}{y_4} \quad (7a)$$

$$\dot{y}_2 = -v_T y_6 \sin(y_5 - y_3) - a_{MR} + y_4 y_1^2 \quad (7b)$$

$$\dot{y}_3 = y_1 \quad (7c)$$

$$\dot{y}_4 = y_2 \quad (7d)$$

$$\dot{y}_5 = y_6 \quad (7e)$$

$$\dot{y}_6 = 0 \quad (7f)$$

Since the filter is implemented on a digital computer, the tracking equations will be cast in discrete form. For this purpose, Eqs. (7) must be integrated across the sampling interval

$$I_k = [t_k, t_{k+1}] \quad (8)$$

where  $t_k$  denotes the  $k$ th sampling time. Fortunately, this integration can be carried out in closed form by integrating in a Cartesian reference frame and subsequently transforming the results to the polar coordinates given in Eq. (6). This approach was used in Ref. 12 for nonmaneuvering targets. Details of the derivation for the system [Eqs. (7)] are given in Ref. 15. Thus, one obtains the discrete equations of motion in the following form:

$$y(k+1) = f[y(k), T] \quad \in R^n \quad (9)$$

where  $n$  is the number of states and

$$y(j) = y(t_j) \quad (10)$$

$$T = t_{k+1} - t_k \quad (11)$$

The measurement equation is

$$m(k) = C(k)y(k) + s(k) \quad \in R^r \quad (12)$$

where  $r$  is the number of measurements,  $C \in R^{r \times n}$  is the measurement matrix, and  $s(k) \in R^r$  is a zero-mean Gaussian white measurement noise with covariance matrix  $S(k) \in R^{r \times r}$ . For bearing rate-only measurements, Eq. (12) is a scalar equation with the measurement matrix

$$C(k) = (1 \ 0 \ 0 \ 0 \ 0 \ 0) \quad (13)$$

The basic tracking algorithm (BTA) is the EKF based on the model [Eqs. (9)–(13)]. The complete set of filter equations and further details can be found in Refs. 1, 15, and 16. For later use, we will give here only the propagation equations of the estimated  $6 \times 6$  covariance matrix  $P$  of the estimation errors associated with the state vector [Eq. (6)]

$$P(k+1/k) = W(k+1,k)P(k/k)W^T(k+1,k) \quad (14)$$

$P(k+1/k)$  is the propagated (a priori) value of  $P$  at time  $t_{k+1}$ ,  $P(k/k)$  is the updated (a posteriori) value of  $P$  at time  $t_k$ , and  $W(k+1,k)$  is the transition matrix associated with the linearized dynamics [Eq. (9)] across the sampling interval  $I_k$ .

#### Observability Results

As mentioned before, the measurement [Eq. (13)] does not guarantee complete observability of the state [Eq. (6)]. This has been analyzed in Refs. 1 and 15. The main conclusions concerning the estimation of the target acceleration are summarized in the following:

1) It can be shown that practically only the target acceleration component  $a_{T\varphi}$  is observable via bearing rate-only (or bearing angle-only) measurements.  $a_{TR}$  is unobservable.

2) In contrast to the range and the range rate,  $a_{T\varphi}$  remains observable even for vanishing bearing rate. This result is of great practical importance because it ensures the availability of  $a_{T\varphi}$  estimates on the homing path, which is characterized by the nominal condition  $\varphi = 0$ .

3) Since  $a_{TR}$  is unobservable, the implementation of guidance laws that use this quantity is useless. However, it is simple to see that  $a_{T\varphi}$  is sufficient information to keep the missile on the homing path, thus ensuring intercept. This follows immediately by linearizing the intercept equations around the homing path. The associated nominal missile control is

$$a_{M\varphi} = a_{T\varphi} \quad (15)$$

In order to stabilize the nominal path, proportional navigation<sup>17</sup> may be used yielding the following guidance law:

$$a_{M\varphi} = a_{T\varphi} - \lambda \dot{R} \dot{\varphi} \quad (16)$$

For a detailed derivation of Eq. (16), see Ref. 15. The guidance law [Eq. (16)] will be referred to as extended proportional navigation (EPN). This guidance law will be used in the simulations in Section VI. Notice that EPN is robust with respect to estimation errors in the unobservable acceleration  $a_{TR}$  because this quantity is not explicitly used in Eq. (16). Only estimates of the observable quantity  $a_{T\varphi}$  are required.

### III. Adaption Scheme

In this section, an adaption scheme is suggested that stabilizes the BTA in the presence of time varying target maneuvers.

#### Derivation of the Adaption Algorithm

As mentioned earlier, the filter produces modeling errors if the target acceleration is not constant. For a constant-speed target, such a maneuver is described by

$$\dot{y}_6 = g(t) \quad (17)$$

where  $g(t)$  is some unknown function of time. Consider the sampling interval  $I_k$  according to Eq. (8). Let  $y(k/k)$  denote the a posteriori state estimate at the time  $t_k$ , based on all past measurements including  $m_k$ , and let  $y(k+1/k)$  denote the a priori state estimate at  $t_{k+1}$ . Assuming that  $y(k/k)$  is exact, the predicted value of  $y_6$  at time  $t_{k+1}$  based on the assumption [Eq. (7f)] is

$$y_6(k+1/k) = y_6(k/k) \quad (18)$$

The resulting propagation error in  $y_6(k+1/k)$  is

$$py_6(k+1) = y_6(k+1) - y_6(k+1/k) = \int_{t_k}^{t_{k+1}} g(\tau) d\tau \quad (19)$$

Obviously,  $py_6$  induces propagation errors  $py_i$ ,  $i = 1, \dots, 5$  in the states  $y_i$  due to the coupling of the dynamics via  $f$  in Eq. (9). The propagation errors

$$py^T = (py_1, \dots, py_6) \quad (20)$$

must be taken into account when solving the covariance equation [Eq. (14)]. Otherwise, the estimated error variances  $p_{ii}$  (diagonal terms of  $P$ ) become smaller than the true variances. The filter overestimates its estimation accuracy. As a consequence, the filter gains tend to zero and the update process of the EKF halts. The filtering reduces to pure propagation resulting in divergence due to the wrong target model used in Eq. (9). A simple way of stabilizing the filter is the modeling of  $py$  as a zero-mean Gaussian white input noise with covariance matrix

$$Q(k) = \text{diag}[q_i(k)], \quad i = 1, \dots, n = 6 \quad (21)$$

For an appropriate selection of  $Q$ , the estimated error variances can be kept larger than the true values, thus avoiding the divergence of the filter. A common choice for  $Q$  is constant values for the  $q_i$ . However, these elements must be chosen large enough to account for the highest possible propagation errors. In most situations, this choice is too conservative because the actual changes of the target maneuver may be lower than assumed when selecting  $Q$ . The estimated error variances then become too large causing considerable estimation errors. It is, therefore, important to adapt the input noise levels  $q_i$  to the actual size of the propagation errors. This procedure is called covariance matching.<sup>3,4</sup> It is based on monitoring the measurement residual

$$r(k+1) = m(k+1) - C(k+1)y(k+1/k) \quad (22)$$

The propagation errors in any observable state result in a deviation of the true statistics of the residual from the statistics computed by the filter. This deviation may be used to estimate  $Q$  such that the consistency of the true and the computed statistics is approximately reestablished.

In order to analyze the statistical properties of  $r$ , the measurement  $m$  according to Eq. (12) is substituted into Eq. (22) yielding

$$r(k+1) = C(k+1)[y(k+1) - y(k+1/k)] + s(k+1) \quad (23)$$

Let

$$e(k+1/k) = y(k+1) - y(k+1/k) \quad (24)$$

denote the true estimation error and  $e^0$  the estimation error in the absence of propagation errors. Hence,

$$y(k+1) = y(k+1/k) + e^0(k+1/k) + py(k+1) \quad (25)$$

Substituting Eq. (25) into Eq. (23) yields

$$r(k+1) = C(k+1)[e^0(k+1/k) + py(k+1)] + s(k+1) \quad (26)$$

To continue the analysis, the following assumptions, which are part of the stochastic model of the propagation errors, are required

$$E[py(k)] = 0 \quad (27a)$$

$$E[e^0(k+1/k)py^T(k+1)] = 0 \quad (27b)$$

$$E[py(k+1)s(k+1)] = 0 \quad (27c)$$

$E[\cdot]$  denotes the expectation conditioned on all past measurements. Notice that with Eq. (27a) the measurement residual is assumed bias free. The residual covariance then becomes

$$\begin{aligned} M(k+1) &= E[r(k+1)r^T(k+1)] = C(k+1) \\ &\times P^0(k+1/k)C^T(k+1) + C(k+1)E[py(k+1) \\ &\times py^T(k+1)]C^T(k+1) + S(k+1) \end{aligned} \quad (28)$$

where

$$P^0(k+1/k) = E[e^0(k+1/k)e^{0T}(k+1/k)] \quad (29)$$

is the solution of Eq. (14).  $P^0$  is the propagated error covariance based on the model [Eq. (7f)]. The associated residual covariance computed by the filter is

$$M^0(k+1) = C(k+1)P^0(k+1/k)C^T(k+1) + S(k+1) \quad (30)$$

Matching  $M$  and  $M^0$  requires the correction of  $P^0$  by

$$Q(k+1) = E[py(k+1)py^T(k+1)] \quad (31)$$

where

$$E[py_i(k+1)py_j(k+1)] = 0 \quad \forall i \neq j \quad (32)$$

is assumed in view of Eq. (21). Hence, the corrected value of  $P$  is

$$P(k+1/k) = P^0(k+1/k) + Q(k+1) \quad (33)$$

Equations (31-33) establish the connection between the modeling errors and the propagated covariance matrix. An equation for  $Q$  is found by substituting Eqs. (30) and (31) into Eq. (28), rendering

$$C(k+1)Q(k+1)C^T(k+1) = M(k+1) - M^0(k+1) \quad (34)$$

Since  $M(k+1)$  is unknown, it is replaced by the sample covariance of the  $N$  most recent residuals

$$M(k+1) \approx \bar{M}(k+1) = \sum_{i=k+1-N}^{k+1} r(i)r^T(i)/(N-1) \quad (35)$$

For the measurement matrix [Eq. (13)], Eq. (34) is a scalar equation for the  $n = 6$  unknowns  $q_i$ . Further specifications to the stochastic model of the propagation errors must be made to eliminate the superfluous unknown quantities. The elimination is based on a coarse estimation of the magnitude of the errors  $py_1, \dots, py_5$  in terms of  $py_6$ . An approximate relationship between the components of  $py$  can be found by linearizing Eq. (9) around the updated state estimate  $y(k/k)$ . This results in

$$|py_i(k+1)| \approx |w_{i6}(k+1,k)||py_6(k+1)|, \quad i = 1, \dots, 6 \quad (36)$$

with

$$w_{i6}(k+1,k) = \frac{\partial f_i(y(k/k), T)}{\partial y_6(k/k)} \quad (37)$$

It should be noted that Eq. (36) must not be used to compute the off-diagonal elements of  $Q$  in Eq. (31) instead of using the assumption [Eq. (32)]. The reason is that Eq. (36) does not contain accurate information about the correlation among the components of  $py$ . An elaboration of this point is outside the scope of this paper. For a detailed derivation of Eq. (36), see Ref. 15.

According to Eqs. (27) and (32), the propagation errors are modeled as uncorrelated white noise processes. The noise intensity associated with the process  $py_6$  is  $\sqrt{q_6}$ . Hence, the stochastic model for  $py_i$  is

$$py_i(k+1) = |w_{i6}(k+1,k)|\sqrt{q_6(k+1)}\eta_i(k+1) \quad (38a)$$

for  $i = 1, \dots, 6$  with

$$\eta_i(k) \sim N(0,1) \quad (38b)$$

$$E[\eta(k)\eta^T(j)] = I_{6 \times 6}\delta_{kj} \quad (38c)$$

where  $I_{6 \times 6}$  is a  $6 \times 6$  identity matrix and  $\delta_{kj}$  denotes the Kronecker delta. Substituting Eqs. (38) into Eq. (31) renders

$$Q(k+1) = \text{diag}[w_{i6}^2(k+1,k)]q_6(k+1) \quad (39)$$

Thus, the estimation of  $Q$  has been reduced to the determination of a single parameter  $q_6$ , which is obtained by the substitution of Eq. (39) into Eq. (34). With  $C(k+1)$  from Eq. (13), this results in

$$q_1(k+1) = \bar{M}(k+1) - p_{11}^0(k+1/k) - S(k+1) \quad (40)$$

$p_{ij}^0$  are the elements of  $P^0$ . With Eq. (39) one obtains

$$q_6(k) = q_1(k)/w_{16}^2(k+1,k) \quad (41)$$

In principle, the adaption at time  $t_{k+1}$  can now be performed by first computing  $q_1(k+1)$  from the known values  $\bar{M}(k+1)$ ,  $p_{11}^0(k+1/k)$ , and  $S(k+1)$ , then using Eqs. (41) and (39) to compute  $Q(k+1)$ , which is used to correct  $P^0$  according to Eq. (33). Via the corrected values of the propagated covariance matrix  $P(k+1/k)$ , the propagation errors are taken into account during the state update of the BTA. However, the following modifications are necessary to keep the adaption scheme stable:

1) By definition,  $Q$  is positive semidefinite. Hence,  $q_1(k+1)$  in Eq. (40) must be  $\geq 0$ . This is ensured by replacing Eq. (40) with

$$\begin{aligned} q_1(k+1) &= q_1'(k+1) \\ &:= \max[0, \bar{M}(k+1) - p_{11}^0(k+1/k) - S(k+1)] \end{aligned} \quad (42)$$

2) If  $w_{16}$  in Eq. (41) tends to zero,  $Q$  becomes infinite. This will occur when the target heading rate is unobservable.<sup>1,15</sup> The error variances will then grow without bounds, indicating complete uncertainty in the state estimates. This behavior is physically meaningful because no information about the propagation errors is available in the measurements. However, typically, the sensitivity  $w_{16}$  vanishes only during short periods on a trajectory and then assumes nonzero values again due to changes of the target maneuver and the intercept geometry. During the intervals of low observability, unrealistically high values of  $Q$  and, hence, the covariance  $P$  should be avoided to ensure filter convergence on subsequent arcs with improved

observability of  $y_6$ . A straightforward approach is the limitation of  $q_6$  by  $q_{6\max}$  and the suppression of adaption when  $p_{66}^0(k+1/k)$  crosses an upper bound  $p_{66\max}$ .

With these modifications, one obtains

$$q_6(k+1) = \min\{q_{6\max}, \max[0, q_1'(k+1)]/w_{16}^2(k+1, k)\} \quad (43a)$$

$$q_6(k+1) = 0 \quad \text{if } p_{66}^0(k+1/k) > p_{66\max} \quad (43b)$$

$q_{6\max}$  is a measure of the maximum possible propagation error per sampling interval associated with the target heading rate. It is bounded by the maximum target heading acceleration  $\gamma_{T\max}$ . A good approximation for  $q_{6\max}$  is

$$q_{6\max} = \ddot{\gamma}_{T\max}^2 T^2 \quad (44)$$

with  $T$  according to Eq. (11).  $p_{66\max}$  approximates the maximal quadratic estimation error in  $y_6$  and is a tuning parameter of the adaption algorithm.

#### Remarks

The output of the adaption algorithm is the matched covariance matrix  $P(k+1/k)$ . This matrix is input to the update equations of the BTA where the propagation errors are corrected by appropriate weighting of the new measurement.

It is evident from Eq. (42) that the variance  $S$  of the measurement noise determines the sensitivity of the adaption scheme with respect to the propagation errors. For large values of  $S$ , the variance  $q_1$  will only become nonzero for large values of  $\dot{M}$ . Hence, adaption will only occur for high propagation errors that, in turn, may lead to filter divergence. On the other hand, adaption will be activated at low levels of the propagation errors for low values of  $S$ . Via Eq. (33), this results in high error variances  $p_{ii}$ , and the state estimates become increasingly noisy and inaccurate for decreasing values of  $S$ . In view of its influence on the adaption algorithm,  $S$  should be considered a tuning parameter (especially if the true measurement noise is unknown). The selection of  $S$  is a trade-off between sufficient sensitivity (which is necessary to adapt to changes of the target acceleration) and estimation accuracy.

There are two mechanisms involved in the estimation of time varying target accelerations. First, a change of the acceleration is detected via Eq. (42) and subsequently tracked via the state update. Note that both mechanisms are integrated in one filter adding a minimum amount of computations to the BTA. In contrast, the multiple model approaches involving different target models result in filter banks with extreme requirements for both computation time and storage.<sup>2,5-7</sup> In other approaches, the detection algorithm is tuned to detect jumps in the target acceleration.<sup>2,8,9</sup> Although these schemes are able to detect abrupt changes of the target maneuver, they usually exhibit low tracking performance after detection and in the presence of smooth, time varying acceleration profiles.

A drawback of the adaption scheme proposed here, is the high sampling rate that is obviously required to track fast changes of the target maneuver. In the following sections, an approach is presented that allows the decoupling of the fast target dynamics from the comparatively slow relative position dynamics. This yields a computationally efficient implementation of the tracking algorithm.

#### IV. Scaling of the Tracking Equations

In this section, a scaled representation of the tracking equations is introduced. The scaling serves the identification of fast and slow states in the dynamic system. The occurrence of fast and slow processes allows for an approximate analysis of the tracking problem in two different time scales: a slow and a fast time scale. The slow and fast states are approximately decoupled in each time scale. Hence, the original problem may be

broken into two lower order subproblems in the slow and fast time scales, respectively. The order reduction is the key to the construction of a computationally efficient tracking algorithm.

The following observations lead to a scaled representation of the tracking equations: 1) the target heading dynamics are much faster than the position dynamics, and 2) the bearing rate is very low. Therefore, the acceleration terms in Eq. (7a) are dominant. Notice that on the homing path the bearing rate nominally vanishes.

These characteristics become explicit in the following singularly perturbed form of the tracking equations:

Slow variables:

$$y_S^T = (y_{12}, y_2, y_3, y_4) \quad (45a)$$

with

$$\dot{y}_{12} = -2(y_1 y_2)/y_4 \quad (45b)$$

$$\dot{y}_2 = -v_T y_6 \sin(y_5 - y_3) - a_{MR} + y_4 y_1^2 \quad (45c)$$

$$\dot{y}_3 = y_1 \quad (45d)$$

$$\dot{y}_4 = y_2 \quad (45e)$$

Fast variables:

$$y_F^T = (y_{11}, y_5, y_6) \quad (46a)$$

with

$$\epsilon \dot{y}_{11} = [v_T y_6 \cos(y_5 - y_3) - a_{Me}]/y_4 \quad (46b)$$

$$\epsilon \dot{y}_5 = y_6 \quad (46c)$$

$$\epsilon \dot{y}_6 = \dot{a}_T(t)/v_T \quad (46d)$$

where  $\epsilon$  is a formal scaling parameter. Notice that

$$y_1 = y_{11} + y_{12} \quad (47)$$

i.e., the bearing rate consists of a slow part  $y_{12}$  and a fast part  $y_{11}$ . It is obvious that for  $\epsilon \ll 1$  changes in the fast variables occur much faster than changes in the slow variables. A rigorous derivation of this scaling with an estimate for  $\epsilon$  is given in Ref. 15. In the next section, the time scale separation inherent in the representation [Eqs. (45-47)] of the tracking dynamics will be used to decouple the estimation of the slow variables  $y_S$  from the estimation of the fast variables  $y_F$ . In this way, a drastic reduction of the number of computations of the tracking algorithm is achieved.

#### V. Design of a Two-Time-Scale Adaptive Tracking Algorithm

##### Outline of the Design Procedure

The decoupling of the estimation of  $y_S$  and  $y_F$  is based on a result for singularly perturbed linear stochastic systems.<sup>13-16</sup> If  $y_S$  and  $y_F$  are the slow and fast states of a linear stochastic system, the full-order Kalman filter associated with the state vector  $y^T = (y_S^T, y_F^T)$  may be approximated by two low-order filters: a slow filter in the slow time scale associated with the slow states  $y_S$  and a fast filter in the fast time scale associated with the fast states  $y_F$ . The slow filter is designed by assuming that the fast states are quasistationary in the time scale of the slow variables. Provided that the fast subsystem is stable, the fast variables may then be expressed in terms of the slow variables. The slow filter is the Kalman filter based on the resulting reduced-order dynamical model for  $y_S$ . In the time scale of the fast variables, the slow states are assumed to be constant. The fast filter is the Kalman filter for the reduced-order dynamics of  $y_F$  in the fast time scale. It can be shown

that the reduced-order filters are a  $\mathcal{O}(\sqrt{\epsilon})$  approximation of the full-order Kalman filter. For more details, see Refs. 13–16.

#### Application to the Tracking Problem

Before applying this procedure to the tracking problem [Eqs. (45–47)], some comments are necessary. Principally, the results known from singularly perturbed linear stochastic systems do not apply to EKF for scaled nonlinear systems because, after linearization of the nonlinear system dynamics and/or the measurement equations around the current state estimate, the resulting system and measurement matrices are themselves stochastic quantities. The main consequence is that the EKFs that are obtained by linearizing the reduced-order systems obtained from Eqs. (45) and (46) are not  $\mathcal{O}(\sqrt{\epsilon})$  approximations to the EKF based on the full-order system dynamics. However, since the full-order EKF is itself only an approximation to the exact nonlinear infinite dimensional filter, it is not meaningful to seek its formally strict  $\mathcal{O}(\sqrt{\epsilon})$  approximation. Instead, a structure for a two-time-scale filter is assumed based on the qualitative results known from singularly perturbed linear systems. The validity of the design must then be tested by simulations as necessary for any EKF.

There is another difficulty when applying the procedure of decoupled filter design. It arises from the fact that the fast subsystem [Eqs. (46)] associated with  $y_F$  is unstable. Therefore, no quasistationary solution in the slow time scale exists and, hence, an order reduction in the slow time scale is impossible. However, in the fast time scale the slow variables may be assumed constant. Therefore, a reduced-order fast filter may be designed. The information produced by the fast filter (FF) is used to decouple the estimation of the slow variables from the dynamics of the fast subsystem. Basically a full-order slow filter (FS) is used in the slow time scale while FF performs the adaption via covariance matching with respect to the measurement residuals in the fast time scale. In this way, FS may be stabilized in the presence of variable target maneuvers without its sampling rate being dictated by the fast dynamics. The FF may be viewed as a predictor for the propagation errors in the slow time scale.

The main modules of the two-time-scale adaptive tracking filter (TATF) are a FS, an adaption algorithm (AA), and a FF. FS is essentially the basic tracking algorithm BTA discussed in Sec. II supplemented by a covariance matching procedure described later. FS operates in the slow time scale with a low sampling rate. The FF is an EKF based on the reduced-order state vector [Eq. (46a)] and is operated with a high sampling rate in order to track fast fluctuations of the fast states. FF is stabilized by the AA presented in Sec. III. The structure of the TATF is depicted in Fig. 2. In the following, the basic operations within one sampling interval in the slow time scale will be described. For clarity, the main parameters of each module are summarized in Tables 1 and 2.

Consider now the slow and the fast time scales depicted in Fig. 3. Let  $t_k$  and  $t_j$  denote the sampling times in the slow and the fast time scales, respectively. The sampling period of FS is selected a multiple of  $T_F$ :

$$T_S = NT_F \quad (48)$$

**Table 1 Parameters of the slow filter**

State vector	$y_S^T = (y_1, \dots, y_6)$
Covariance matrices	$P_S, Q_S$
Sampling period	$T_S$

**Table 2 Parameters of the fast filter**

State vector	$y_F^T = (y_{11}, y_5, y_6)$
Covariance matrices	$P_F, Q_F$
Sampling period	$T_F$

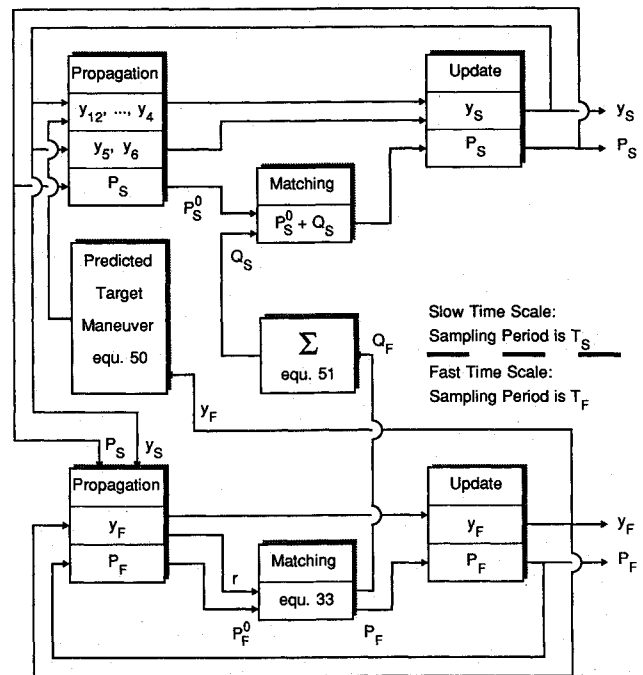


**Fig. 2 Structure of the TATF.**

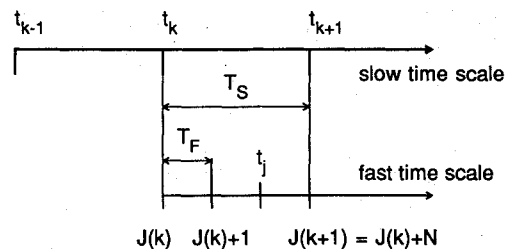


**Fig. 3 Time scales of the TATF.**

The sampling times  $t_j$ ,  $j = J(k), \dots, J(k+1)$  within the sampling interval  $I_k = [t_k, t_{k+1}]$  are chosen such that

$$t_{J(k)} = t_k \quad (49a)$$

$$t_{J(k+1)} = t_{k+1} \quad (49b)$$

with

$$J(k+1) = J(k) + N \quad (49c)$$

Equations (49) are the synchronization equations of FF and FS. The operating sequence of the TATF is now as follows. First, FF is run from  $t_{J(k)}$  to  $t_{J(k+1)}$ . Based on the measurements at the sampling times  $t_j$ , the filter produces an estimate of the target maneuver in  $I_k$  given by the a posteriori estimates

$$y_5(j/j) \text{ and } y_6(j/j), \quad j = J(k), \dots, J(k+1) \quad (50)$$

Time varying target maneuvers are detected and tracked using the AA. The AA produces estimates of the propagation errors in each subinterval  $I_j = [t_j, t_{j+1}]$  in terms of the covariance matrix  $Q_F(j)$ ,  $j = J(k), \dots, J(k+1)$ . The FS is started after FF reaches the sampling time  $t_{k+1}$ . Provided that FF converges on  $I_k$ , the estimated target maneuver [Eq. (50)] will be more accurate than the estimate based on the model [Eq. (7f)] implemented in FS. Therefore, the slow variables  $y_{12}, \dots, y_4$  are propagated using the maneuver [Eq. (50)] predicted by FF. As a result, the a priori estimates  $y_i(k+1/k)$ ,  $i = 1, \dots, 4$  at the time  $t_{k+1}$  do not contain any significant propagation errors. The accuracy of the estimates  $y_5$  and  $y_6$  produced by FF

at the time  $t_{k+1}$  may be improved by reestimating these states in the slow time scale. In this way, the variation of the slow states that are considered constant by FF can be taken into account. The reestimation involves solving the propagation equations for  $y_5, y_6$  based on the model [Eq. (7f)]. The resulting propagation error is then corrected via covariance matching in the slow time scale. This is possible because the predicted propagation error is available via the covariances  $Q_F(j)$ . Using the noise model introduced in Sec. III, a measure for the predicted propagation error at  $t_{k+1}$  is

$$Q_S(k+1) = \text{diag}(q_{Si}(k+1)), \quad i = 1, \dots, 6 \quad (51)$$

with

$$q_{Si}(k+1) = 0, \quad i = 1, \dots, 4 \quad (52)$$

$$q_{Si}(k+1) = \sum_{j=J(k)+1}^{J(k+1)} q_{Fi}(j), \quad i = 5, 6 \quad (53)$$

The matching is performed by correcting the propagated error covariance matrix  $P_S(k+1/k)$  by  $Q_S(k+1)$  according to Eq. (33) prior to solving the update equations of the BTA (see Sec. II). Notice that no adaption is necessary for the states  $y_i$ ,  $i = 1, \dots, 4$  because they are propagated based on the predicted maneuver [Eq. (50)]. This explains Eq. (52).

### Discussion

The matching of the covariance matrices  $P_F$  and  $P_S$  with respect to the measurement residuals in the fast time scale is the essential mechanism that results in the decoupling of the fast and slow dynamics. The decoupling is possible because the propagation errors are produced in the fast time scale. Since the dimension of FF is very low compared to FS, the sampling rate in the fast time scale may be chosen much higher than achievable for FS. This becomes evident by comparing the number of propagation equations of FS and FF. For FS, the number of propagation equations is 21 (6 states and 15 elements of  $P_S$ ), whereas the number is 6 (3 states and 3 elements of  $P_F$ ) for FF.

The assumption of constant values for the slow variables in FF is justified during short periods of time because the rate of change of these variables is very low compared to the fast variables. However, this assumption is not valid for the total problem duration. Therefore, the values of the slow variables in FF must be updated periodically to keep the FF from diverging. This update procedure includes reinitializing the fast states  $y_F$  and the associated covariance matrix  $P_F$ . All quantities are updated with their latest estimates provided by the FS at the sampling times  $t_k$ . For details of the synchronization of FS and FF see Ref. 15.

## VI. Simulation Results

In this section, simulation results are presented that were obtained by filtering data of a short range intercept scenario.

### Intercept Scenario

The intercept geometry is shown in Fig. 4. Missile and target start with zero heading angle with respect to the initial line of sight. The initial range is 3.5 km. The motion takes place in a horizontal plane. The missile guidance law is EPN (see Sec. II). The target maneuvers with zero lateral acceleration  $a_T$  from the initial time  $t_0 = 0$  to  $t_e = 2.5$  s. At the time  $t_e$ , the acceleration changes abruptly from  $a_T = 0$  to  $a_T = 9$  g and subsequently decreases linearly to  $a_T = 6$  g at final time  $t_f = 9$  s. The target speed is  $v_T = 270$  m/s. As mentioned in Sec. II,  $v_T$  is a parameter of the filter that is assumed to be known. In order to account for uncertainties in this parameter, the subsequent simulation results are based on a target speed that is 10% below the true value. The main parameters of the filter are presented in Table 3.

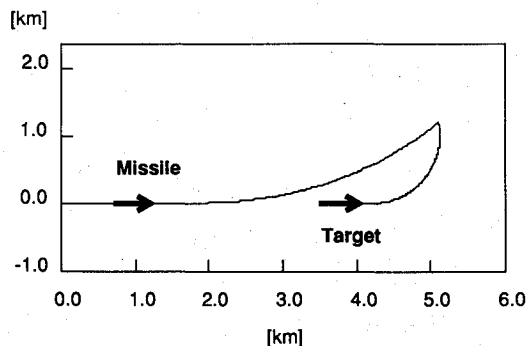


Fig. 4 Intercept Geometry.

Table 3 Main parameters of the filter

Sampling period in the slow time scale	$T_S = 0.2$ s
Sampling period in the fast time scale	$T_F = 0.04$ s
Window length for residual averaging	$N = 5$
Upper bound for $q_6$ [Eqs. (43) and (44)]	$q_{6\max} = 0.0045 \text{ rad}^2\text{s}^{-2}$
Upper bound for $p_{66}^0$ [Eqs. (43)]	$p_{66\max} = 0.1 \text{ rad}^2\text{s}^{-2}$
Power spectral density of measurement noise	$10^{-6} \text{ rad}^2\text{s}^{-1}$
Initial estimation error of target heading angle	$-0.1$ rad angle
Initial estimation error of target heading rate	$-0.1$ rad/s
Assumed target velocity	$0.9 \times \text{true target velocity}$

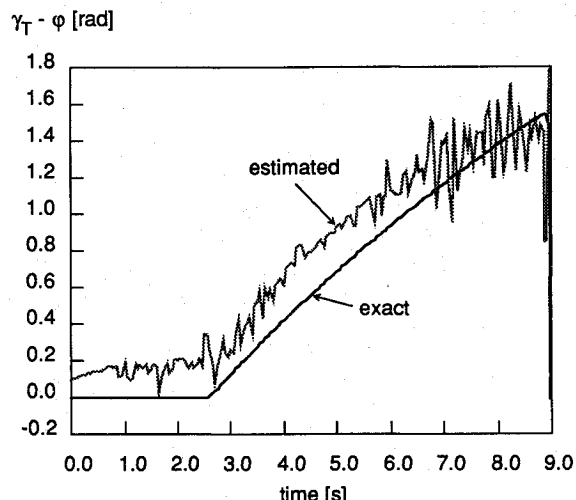


Fig. 5 Exact and estimated target heading with respect to current line of sight.

### Discussion of Results

The target maneuver is determined by the target heading angle and the target heading rate according to Eq. (3). The exact and estimated histories of these quantities are shown in Fig. 5 and 6, respectively. According to Eq. (3), the trajectories in Fig. 6 reflect the exact and estimated target acceleration profiles. It can be seen that the initial estimation error of the heading rate immediately decreases, whereas the heading error remains uncorrected. This is due to the fact that the heading angle is unobservable for zero target acceleration in contrast to the heading rate.<sup>1,15</sup> The jump of the target acceleration at  $t_e$  is detected after a small delay. The delay is unavoidable because the adaption is achieved only after the propagation errors exceed a certain threshold, according to Eqs. (42) and (43). After the detection of the acceleration jump, the heading rate estimates converge to the exact heading rate profile in the second half of the observation interval. The convergence of the heading angle estimates is much slower, which is again due to the low observability in this intercept geometry.<sup>1,15</sup> However, shortly before intercept, good estimates are available.

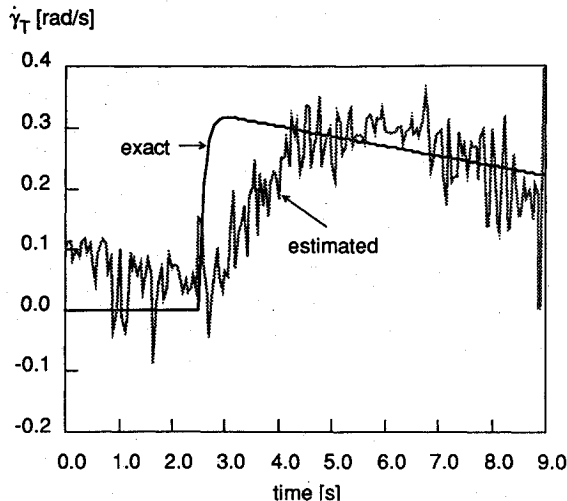


Fig. 6 Exact and estimated target heading rate.

The results demonstrate that the filter maintains its tracking capability after maneuver detection in contrast to other tracking filters based on detection methods (see, for example, Ref. 9). More simulation results for different types of target maneuvers are reported in Refs. 1, 15, and 16.

## VII. Concluding Remarks

In this paper, a new tracking filter for maneuvering targets has been presented. The detection and tracking of time varying target maneuvers is based on a simple covariance matching procedure. An efficient implementation of the filter was obtained by taking advantage of the time scale separation of the tracking dynamics. It allows the construction of a full-order slow filter that operates in the time scale of the slow variables and a reduced-order fast filter operating in a fast time scale. The fast filter performs the monitoring of the residuals necessary for the covariance matching. This is physically meaningful because the modeling errors occur in the fast time scale. In contrast to filters based on a detection approach, the two-time-scale filter presented here maintains its tracking capability after detection of changes of the target maneuver. Since it uses only one model for the target dynamics, it is computationally much more efficient than tracking algorithms based on filter banks.

## Acknowledgment

The authors would like to thank the reviewers for many valuable comments.

## References

- <sup>1</sup>Hepner, S. A. R., and Geering, H. P., "Observability Analysis for Target Maneuver Estimation via Bearing-Only and Bearing-Rate-Only Measurements," *Journal of Guidance, Control, and Dynamics*, Vol. 13, No. 6, 1990, pp. 977-983.
- <sup>2</sup>Chang, C. B., and Tabaczynski, J. A., "Application of State Estimation to Target Tracking," *IEEE Transactions on Automatic Control*, Vol. AC-29, No. 2, 1984, pp. 98-109.
- <sup>3</sup>Jazwinsky, A. H., *Stochastic Processes and Filtering Theory*, Academic Press, New York, 1970.
- <sup>4</sup>Jazwinsky, A. H., "Adaptive Filtering," *Proceedings of the IFAC Symposium on Multivariable Control Systems*, VDI/VDE-Fachgruppe Regelungstechnik, Düsseldorf, Germany, Oct. 1968, pp. 1-15.
- <sup>5</sup>Moose, R. L., and McCabe, D. H., "Applications of Adaptive State Estimation Theory," *Proceedings of the 19th IEEE Conference on Decision and Control*, Inst. of Electrical and Electronics Engineers, Piscataway, NJ, Dec. 1980, pp. 568-575.
- <sup>6</sup>Maybeck, P. S., and Hentz, K. P., "Investigation of a Moving-Bank Multiple Model Adaptive Algorithm," *Journal of Guidance, Control, and Dynamics*, Vol. 10, No. 1, 1987, pp. 90-96.
- <sup>7</sup>Tenney, R. R., Hebbert, R. S. and Sandell, N. R., "A Tracking Filter for Maneuvering Sources," *IEEE Transactions on Automatic Control*, Vol. AC-22, April 1977, pp. 246-251.
- <sup>8</sup>Dowdle, J. R., Athans, M., Gully, S. W., and Willsky, A. S., "An Optimal Control and Estimation Algorithm for Missile Endgame Guidance," *Proceedings of the 21st IEEE Conference on Decision and Control*, Inst. of Electrical and Electronics Engineers, Piscataway, NJ, Dec. 1982, pp. 1128-1132.
- <sup>9</sup>Bowman, G. A., and Speyer, J. L., "Detection Filters for Missile Tracking," *Proceedings of the AIAA Guidance, Navigation, and Control Conference*, AIAA, New York, 1987, pp. 570-578.
- <sup>10</sup>Aidala, V. J., "Kalman Filter Behavior in Bearings-Only Tracking Applications," *IEEE Transactions on Aerospace and Electronic Systems*, Vol. AES-15, July 1979, pp. 29-39.
- <sup>11</sup>Nardone, S. C., and Aidala, V. J., "Observability Criteria for Bearings-Only Target Motion Analysis," *IEEE Transactions on Aerospace and Electronic Systems*, Vol. AES-17, July 1981, pp. 162-166.
- <sup>12</sup>Aidala, V. J., and Hammel, S. E., "Utilization of Modified Polar Coordinates for Bearings-Only Tracking," *IEEE Transactions on Automatic Control*, Vol. AC-28, Aug. 1983, pp. 283-294.
- <sup>13</sup>Haddad, A. H., and Kokotovic, P. V., "On Singular Perturbations in Linear Filtering and Smoothing," *Proceedings of the Symposium on Nonlinear Estimation and its Applications*, Western Periodicals Co., North Hollywood, CA, 1975, pp. 96-103.
- <sup>14</sup>Haddad, A. H., "Linear Filtering of Singularly Perturbed Systems," *IEEE Transactions on Automatic Control*, Vol. AC-21, Aug. 1976, pp. 515-519.
- <sup>15</sup>Hepner, S. A. R., "Analysis of the Planar Intercept and Tracking Problem by Application of Optimal Control and Singular Perturbation Theory," Ph.D. Dissertation, Swiss Federal Institute of Technology, Zürich, Switzerland, 1986.
- <sup>16</sup>Hepner, S. A. R., and Geering, H. P., "Target Acceleration Estimation in Planar Intercept Scenarios," *Proceedings of the AIAA Guidance, Navigation, and Control Conference*, AIAA, Washington, DC, 1988, pp. 84-94.
- <sup>17</sup>Bryson, A. E., and Ho, Y. C., *Applied Optimal Control*, Hemisphere, New York, 1975.